

General Disclaimer

One or more of the Following Statements may affect this Document

- This document has been reproduced from the best copy furnished by the organizational source. It is being released in the interest of making available as much information as possible.
- This document may contain data, which exceeds the sheet parameters. It was furnished in this condition by the organizational source and is the best copy available.
- This document may contain tone-on-tone or color graphs, charts and/or pictures, which have been reproduced in black and white.
- This document is paginated as submitted by the original source.
- Portions of this document are not fully legible due to the historical nature of some of the material. However, it is the best reproduction available from the original submission.

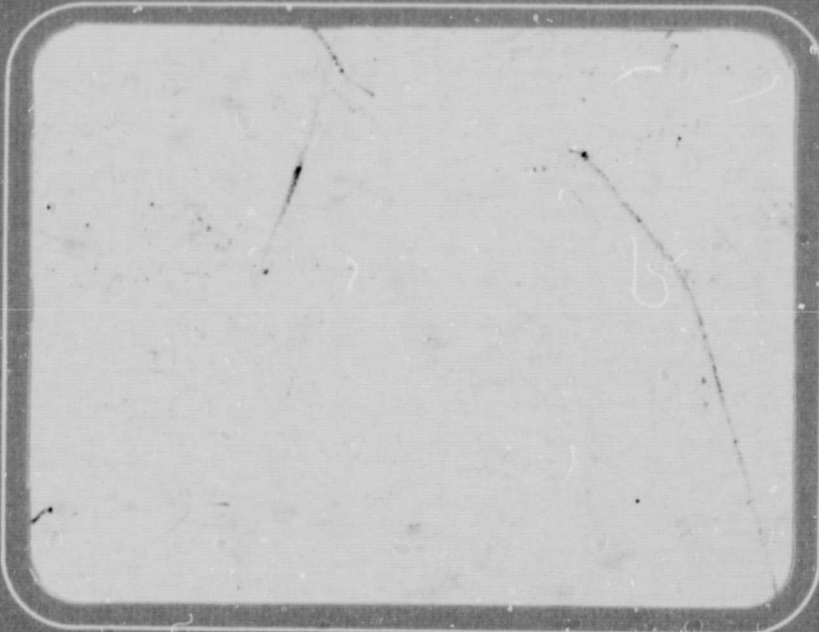
CR-170865



Battelle
Columbus Laboratories



Report



(NASA-CR-170865) EVALUATION OF FEASIBILITY
OF MEASURING EHD FILM THICKNESS ASSOCIATED
WITH CRYOGENIC FLUIDS Final Report
(Battelle Columbus Labs., Ohio.) 34 p
HC A03/MF A01

N83-34084

Unclas

CSSL 20L G3/31 41994

FINAL REPORT

ORIGINAL CONTAINS
COLOR ILLUSTRATIONS

on

Contract NAS 8-34908

EVALUATION OF FEASIBILITY OF MEASURING EHD
FILM THICKNESS ASSOCIATED WITH CRYOGENIC FLUIDS

to

NATIONAL AERONAUTICS AND SPACE ADMINISTRATION
GEORGE C. MARSHALL SPACE FLIGHT CENTER

August 26, 1983

by

J. W. Kannel, T. L. Merriman
R. D. Stockwell, and K. F. Dufrane

BATTELLE
Columbus Laboratories
505 King Avenue
Columbus, Ohio 43201

TABLE OF CONTENTS

	<u>Page</u>
INTRODUCTION	1
CONCLUSIONS	2
NEEDED FURTHER RESEARCH	3
PROJECT DETAILS	4
Lubricant Film Thickness Experiments	4
Description of Disk Apparatus	4
Results of LN ₂ EHD Experiments	9
Extrapolation to SSME Pump Bearings	14
Analysis of Test Bearings	15
Component Inspection	15
Bearing Load Computations	23
Calculating Units	29

LIST OF TABLES

Table 1. Film Thickness Data Obtained With LN ₂	10
Table 2. Summary of Geometry and Operating Conditions for SSME Turbopump Bearing (7955) and Battelle Disk Apparatus	16
Table 3. Identification and Time of Running on Three Bearings From HPOTP Tests	17
Table 4. Assumed Design Conditions for HPOTP Turbine-End Bearings	24

LIST OF FIGURES

Figure 1. Disk Apparatus Used in EHD Film Thickness Experiments	5
---	---

TABLE OF CONTENTS
(Continued)

Page

LIST OF FIGURES
(Continued)

Figure 2.	Contact Stress as a Function of Load for 76.2mm (3 in.) Twin Disks	7
Figure 3.	Liquid Nitrogen Being Injected Into Disk Contact Region	8
Figure 4.	Accuracy of Regression of Film Thickness Data	11
Figure 5.	Regressed Film Thicknesses for Liquid Nitrogen (76.2 mm (3 in.) Diameter Disk) Metric Units	12
Figure 6.	Regressed Film Thicknesses for Liquid Nitrogen (76.2 mm (3 in.) Diameter Disk) English Units	13
Figure 7.	Rolled-Over Shoulder and Band of Spalls on Inner Race of Turbine Bearing No. 3 From Unit 2209R1	18
Figure 8.	Band of Spalls on Outer Race of Turbine Bearing No. 3 From Unit 2209R1	20
Figure 9.	Scalloped Wear Patterns on Outer Race of No. 2 Preburner Bearing From Unit No. 2209R1	21
Figure 10.	Damage From Spinning to the Outer Diameter of the Outer Race of No. 2 Preburner Bearing From Unit No. 2209R1	22
Figure 11.	Contact Angle Variation for SSME HPOTP Bearing (7955) at 30,000 rpm, 3780 N (850 lb) Axial and No External Radial Load	25
Figure 12.	Contact Stress and Length for SSME HPOTP Bearings (7955) at 30,000 rpm, 3780 N (850 lb) Axial and No Radial Load	26
Figure 13.	Contact Angle Variation with Radial Load at Maximum Load Position SSME HPOTP Bearing (7955) at 30,000 rpm and 3780 N (850 lb) Axial Load	27
Figure 14.	Contact Stress and Half-Width Variation with Radial Load at Maximum Load Position for SSME HPOTP Turbo-pump Bearing (7955) at 30,000 rpm and 3780 N (850 lb) Axial Load	

ABSTRACT

The objective of this task was to evaluate the feasibility of measuring elastohydrodynamic (EHD) films as formed with a cryogenic (LN₂) fluid. Modifications were made to an existing twin disk EHD apparatus to allow for disk lubrication with liquid nitrogen. This disk apparatus is equipped with an X-ray system for measuring the thickness of any lubricant film that is formed between the disks. Several film thickness experiments were conducted with the apparatus which indicate that good lubrication films are formed with LN₂. Films as thick as 1 μm (40 μin.) were measured under light load conditions. In addition to the film thickness studies, failure analyses of three NASA-supplied bearings were conducted. The HPOTP turbine-end bearings had experienced axial loads of 36,000 to 44,000 N (8,000 to 10,000 lb). High continuous radial loads had also been experienced, which were most likely caused by thermal growth of the inner race. The resulting high internal loads caused race spalling and ball wear to occur.

EVALUATION OF FEASIBILITY OF MEASURING EHD FILM THICKNESS ASSOCIATED WITH CRYOGENIC FLUIDS

by

J. W. Kannel, T. L. Merriman
R. D. Stockwell, and K. F. Dufrane

INTRODUCTION

In order to capitalize on the success of the space shuttle, it is imperative that efforts be expanded to develop the technology required for maintenance-free reusable systems for at least the target of 7.5 hours. In this regard, the bearings in the space shuttle main engine (SSME) continue to represent a long term problem area. The bearings must operate at very high DN values (1.7×10^6) under poor lubrication conditions. The bearing's lubrication must be derived from transfer of the cage material (PTFE) or from cryogenic hydrogen or oxygen.

Battelle has been assisting NASA in bearing development of the SSME bearings through a task order arrangement. The current Task 110 is complimentary to the previous Task 109. In Task 109, a theoretical model for the lubrication of a ball bearing with a cryogenic fluid was developed. That model was based on classical elastohydrodynamic theory for liquid lubrication. Elastohydrodynamic (EHD) theory involves consideration of the elasticity of the balls and races in conjunction with the hydrodynamics of the liquid lubricant. The model, when applied to ball bearings lubricated with liquid oxygen (LOX), indicated that a very thin layer (i.e., an EHD film) of the LOX might be formed between balls and races. However, the model was very speculative.

The objective of the current task was to evaluate the feasibility of measuring cryogenic EHD films. An existing twin disk apparatus was modified for the experiments to accept liquid nitrogen. The apparatus is equipped with an X-ray system for measuring film formations between the disks. The task involved:

1. Modifying the disk machine to study cryogenic film lubricants.

2. Performing feasibility experiments with the X-ray disk apparatus.
3. Conducting a series of experiments with the disk apparatus.

In addition, three bearings supplied by NASA/MSFC, which had been operated under a liquid oxygen environment, were analyzed.

CONCLUSIONS

As a result of the task, the following conclusions can be made.

1. The use of the Battelle twin disk machine to study lubrication by cryogenic fluids appears to be quite feasible. The apparatus was operated in an LN₂ environment for several experiments. The disks and supply fluid were easily maintained at the same temperature.
2. Lubricating films on the order of 1.07 μm (42 $\mu\text{in.}$) were measured at light loads (.24 GPa (35 ksi)) and 10,000 rpm (20 m/sec (785 ips) surface speed). Even under more severe loads of .41 GPa (60 ksi) films as thick as .56 μm (22 $\mu\text{in.}$) were detected.
3. If the film measurements are extrapolated to an SSME LOX pump bearing operating at a contact pressure of 1.37 GPa (200 ksi), films on the order of .29 μm (11 $\mu\text{in.}$) might be expected. At contact pressures of 2.07 GPa (300 ksi) the film thickness would be on the order of .19 μm (7.6 $\mu\text{in.}$).

4. High axial loads on the turbine-end bearings are still being experienced in both directions. Thermal growth of the inner race is causing extremely high internal radial loads, which are causing spalling and ball wear.

NEEDED FURTHER RESEARCH

Based on the studies conducted in this task, it appears that liquid lubrication with a cryogenic fluid is very feasible. The experiments indicated not only that cryogenic EHD films can be measured, but also that these films may be of sufficient thickness to protect SSME turbopump bearing surfaces under realistic operating conditions. However, since the measurements were obtained under low contact stress conditions, considerable extrapolation was required to evaluate the lubrication in the SSME turbopump bearings. A new task should be conducted which would involve EHD film evaluations under "realistic" bearing stresses.

Specifically, the task should be conducted that involves

1. The measurement of EHD film thickness under contact stress conditions on the order of 1.4-2 GPa (200-300 ksi).
2. The measurement of the electric continuity across the lubricant film to verify the film thickness measurements. In this type of experiment, a large measured resistance indicates good lubrication and substantiates thick film X-ray measurements. Conversely, a low resistance indicates film breakdown.
3. The measurement of traction (friction) between the disk to evaluate the frictional behavior of cryogenic films.

The high stress conditions as indicated by No. 1 above can be achieved either through the use of a smaller diameter disk than used in this task, by modifying the disk by introducing an axial crown, or by decreasing the width. The advantages of using the larger diameter disk is that surface speeds of the type seen in the bearing can be achieved. Techniques are available for measuring electrical continuity (see 2 above) for either size disk.

There are several reasons for obtaining traction measurements (3 above). Friction is, of course, a critical aspect of bearing heating and accurate measurements are needed for complex theoretical models currently being used by NASA. In addition, traction measurements can show considerable insight into the rheology of cryogenic fluids. This rheology is related to EHD film formations and can be used as further substantiation of the film measurements.

PROJECT DETAILS

Lubricant Film Thickness Experiments

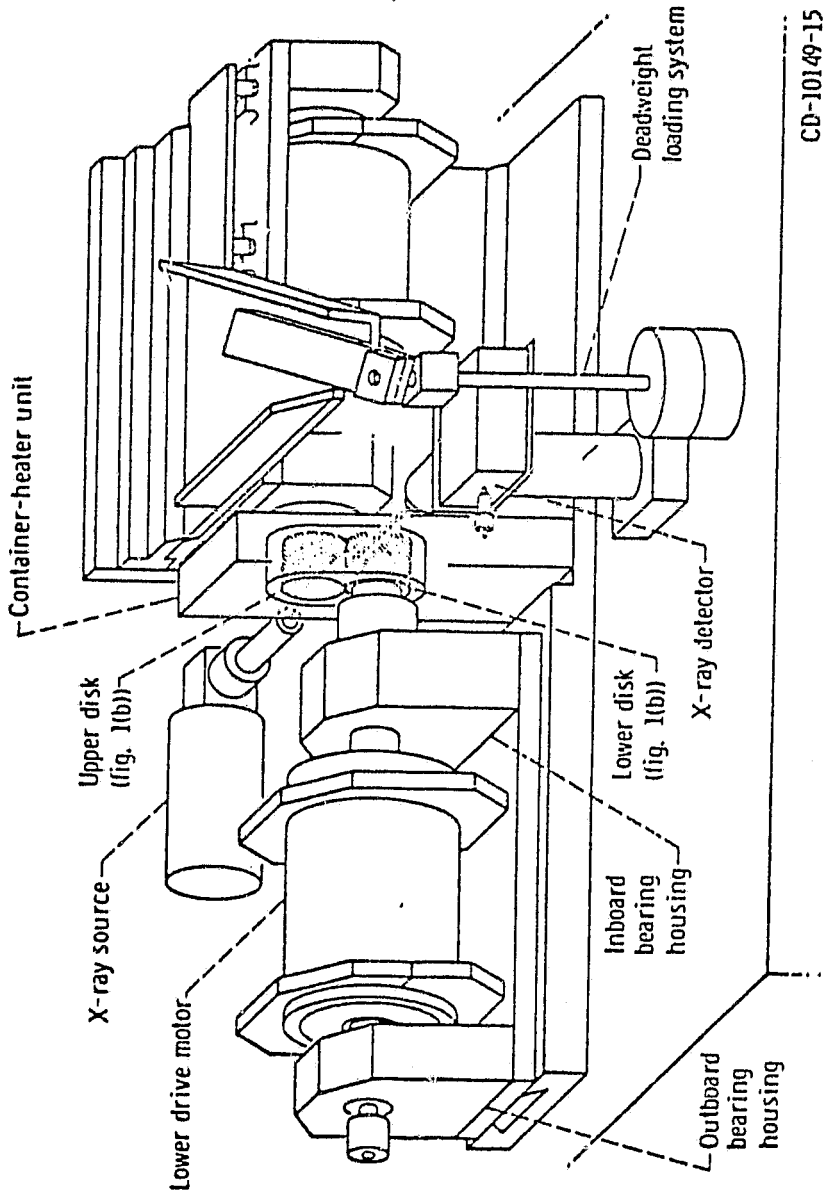
Description of Disk Apparatus

The experiments for the project were conducted with the twin disk apparatus, shown pictorially in Figure 1. The apparatus consists of two disks loaded against each other in rolling contact, each of which are driven by variable frequency induction motors. The shafts of the drive motors are integral with the disk drive shafts and are mounted in duplex ABEC-7 45 mm bearings. The electrical power to the motors is supplied by a variable frequency supply unit. Disk speeds up to 15,000 rpm and continuously variable slip-ratios between the disks can be achieved.

The disks in the experiments were 76.2 mm (3 in.) in diameter by 22.3 mm (.88 in.) wide. These disks were mounted on tapered stub-shafts which fit into the drive shafts.

Loading is achieved by a deadweight system with a mechanical advantage of approximately 12. A pneumatic cylinder is used to support the load

ORIGINAL PAGE 19
OF POOR QUALITY



CD-10149-15

(a) Schematic.

FIGURE 1. DISK APPARATUS USED IN EHD FILM THICKNESS EXPERIMENTS

on the disks until it is desired in an experiment. This pneumatic arrangement also allows quick unloading of the disk when the experiments are terminated. A load-stress curve for the apparatus is given in Figure 2. As an example, a deadweight load of 169 N (38 lb) produces a disk load of 2028.3 N (446 lb) and, hence, a contact stress of .41 GPa (60 ksi).

EHD film thickness is measured by means of a collimated X-ray beam. X-rays pass readily through the LN₂, but find the steel disk quite opaque. By measuring the rate of X-ray transmission, the film thickness (gap) between the disks can be measured.

The twin-disk apparatus has been used in numerous experiments involving "normal" oil lubrication. For those experiments, oil is supplied to the disk through a jet directed at the disk contact region. A recirculating oil supply system is used, which includes a supply pump, a scavenging pump, and a heated (or cooled) oil pump. Normally, the lubricant supply temperature is essentially the same as the disk temperature and very similar to the shaft and bearing temperatures. Disk experiments with cryogenic fluids represented a significant departure from normal operation and concern for overall apparatus operation.

The cryogenic fluid evaluated was liquid nitrogen (LN₂). LN₂ was supplied to the disk on a once-through system using tank pressure to deliver the fluid. LN₂ has a boiling temperature of 77.3K (139.5 R) at ambient pressure while the disk shaft temperature is approximately 322K (580 R). The temperature differential between disk and shaft, then, is at least 245K (440 R). There are several possible problems associated with temperature differentials, such as shaft growth, shaft distortion, and over-cooling the support bearings.

Despite the potential difficulties, the disk apparatus was found to operate in a very stable thermal mode with no significant thermal distortion problems. Temperature was monitored by thermocouples located on the side of both the upper and lower disk and in the jet inlet. All temperatures were identical in all tests. A photograph showing the LN₂ being injected into the disk chamber is shown in Figure 3. For this photograph, the side of the disk housing was removed to allow for visual access. Preliminary experiments revealed that the primary problem with the apparatus was in

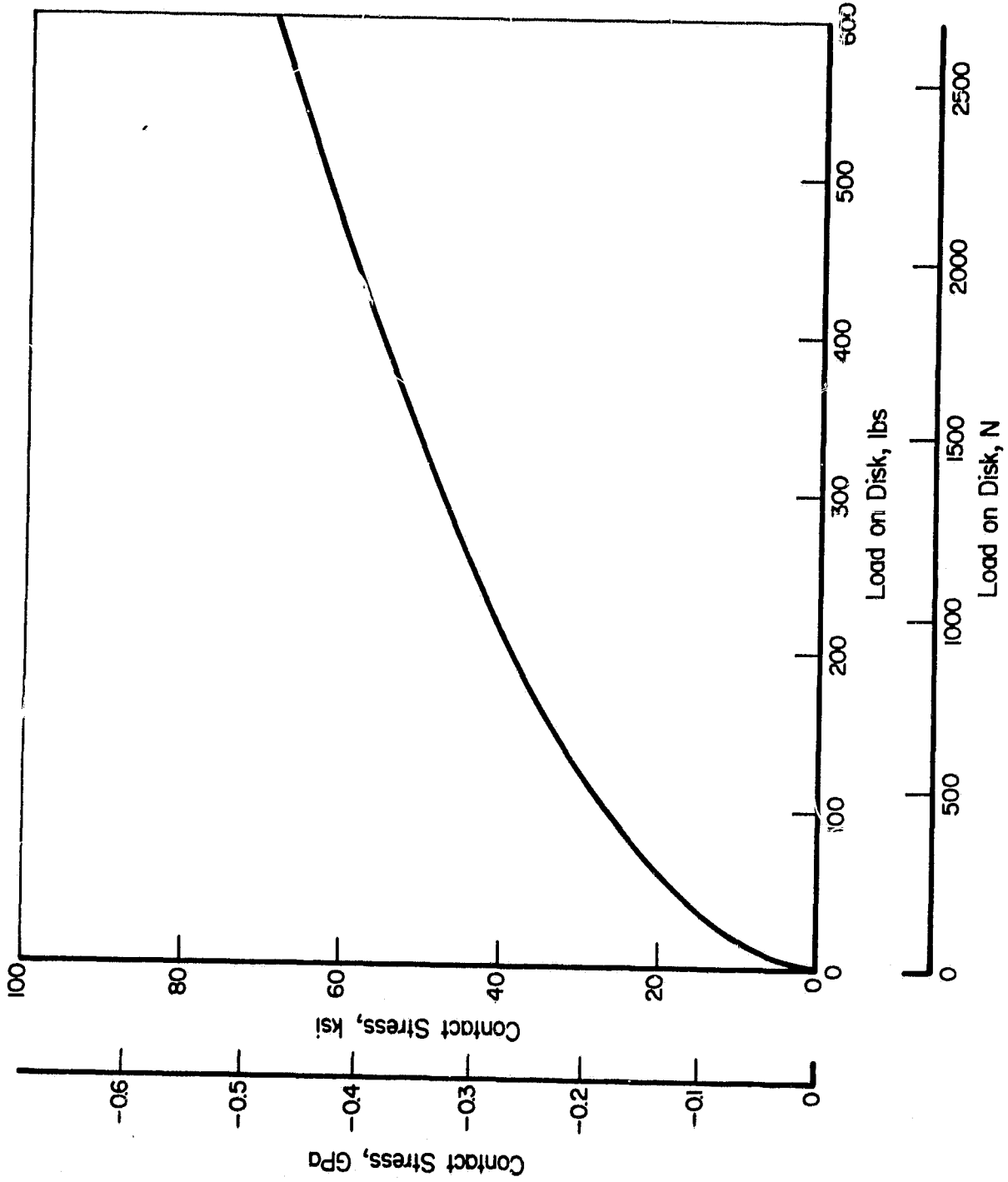


FIGURE 2. CONTACT STRESS AS A FUNCTION OF LOAD FOR 76.2mm (3 in.) TWIN DISKS

ORIGINAL PAGE IS
OF POOR QUALITY

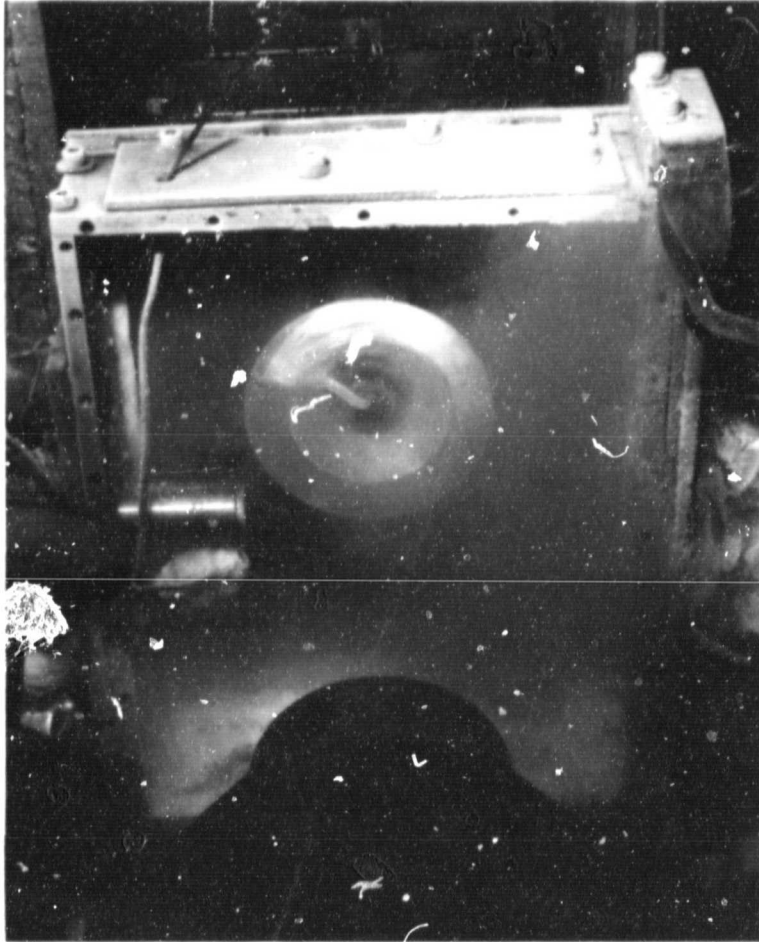


FIGURE 3. LIQUID NITROGEN BEING INJECTED
INTO DISK CONTACT REGION

maintaining liquid nitrogen on the disk surface. If the nitrogen flow was too low, an ice film formed on the disk surface which gave extremely large film thickness indications. To minimize this problem, the disk housing was sealed as tightly as feasible and a "steady" flow of nitrogen was supplied to the disks. Once an experiment had been initiated, the flow was not interrupted until all tests were completed.

Results of LN₂ EHD Experiments

Several film thickness experiments were conducted in the course of the task, as shown in Table 1. Good EHD films were detected for all of the tests. Since the films are typically very thin, small errors ($\sim 5 \mu\text{in.}$ ($.13 \mu\text{m}$)) can cause large scatter in the data. For this reason, a least-squares regression analysis was applied to the data. The results of both the measurements and the regressions are shown in Table 1. The regression accuracy is illustrated in Figure 4. The accuracy is about $.11 \mu\text{m}$ ($4 \mu\text{in.}$).

In general, the film thickness obtained for LN₂ were on the order of $.6 \mu\text{m}$ ($24 \mu\text{in.}$) for the disk experiment (see Figures 5 and 6). The prediction using Equation 3 of our last report, would indicate that the films should be on the order of $.12 \mu\text{m}$ ($5 \mu\text{in.}$). One explanation for the discrepancy is in the disk surface temperature. It was assumed, for the calculations, that the surface temperature was 77K (138 R) (i.e., the boiling temperature of LN₂ at ambient pressure). However, it is possible that the disk surface temperature was colder than 77K. It is also possible that the viscosity of LN₂ increases with pressure which was not considered in the Battelle theory.

Regardless of the explanation for the measured film thicknesses, the significant fact is that a thick EHD film was formed in the disk experiments. To further verify the existence of cryogenic films, more experiments are required and should include:

1. Electrical continuity experiments across the disks to verify the existence of a thick insulating layer.

TABLE 1. FILM THICKNESS DATA OBTAINED WITH LN₂

Speed, rpm	Load N(lb)	Contact Stress GPa (ksi)	Measured Film Thickness μm ($\mu\text{in.}$)	Regressed Film Thickness μm ($\mu\text{in.}$)	Theoretical Film Thickness (77K) μm ($\mu\text{in.}$)
5,000	44.5 (10)	.206 (30)	.71 (28)	.76 (30.1)	.18 (7)
	62.3 (14)	.241 (35)	.56 (22)	.67 (26.1)	.15 (5.8)
	80.0 (18)	.276 (40)	.64 (25)	.60 (23.0)	.13 (5.2)
	98.0 (22)	.310 (45)	.64 (25)	.52 (20.6)	.12 (4.6)
	120.0 (27)	.344 (50)	.46 (18)	.48 (18.7)	.11 (4.2)
10,000	62.3 (14)	.241 (35)	1.07 (42)	.97 (38.0)	.24 (9.6)
	80.0 (18)	.276 (40)	.94 (37)	.84 (33.5)	.22 (8.6)
	98.0 (22)	.310 (45)	.71 (28)	.76 (30.0)	.19 (7.6)
	120.0 (27)	.344 (50)	.64 (25)	.70 (27.2)	.18 (7.0)
	169.0 (38)	.414 (60)	.56 (22)	.59 (23.0)	.15 (5.8)

LIQUID NITROGEN

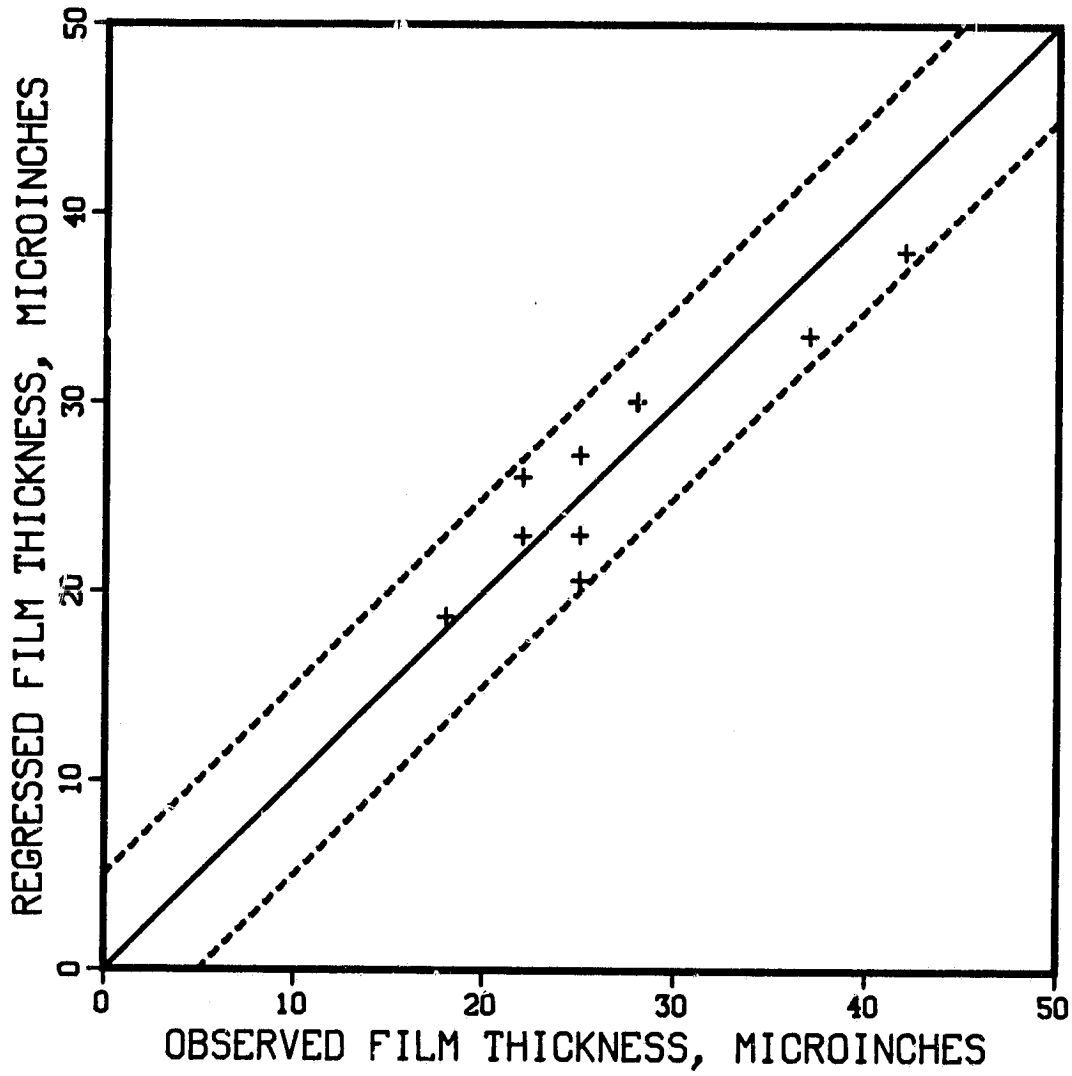


FIGURE 4. ACCURACY OF REGRESSION OF FILM THICKNESS DATA

ORIGINAL PAGE IS
OF POOR QUALITY

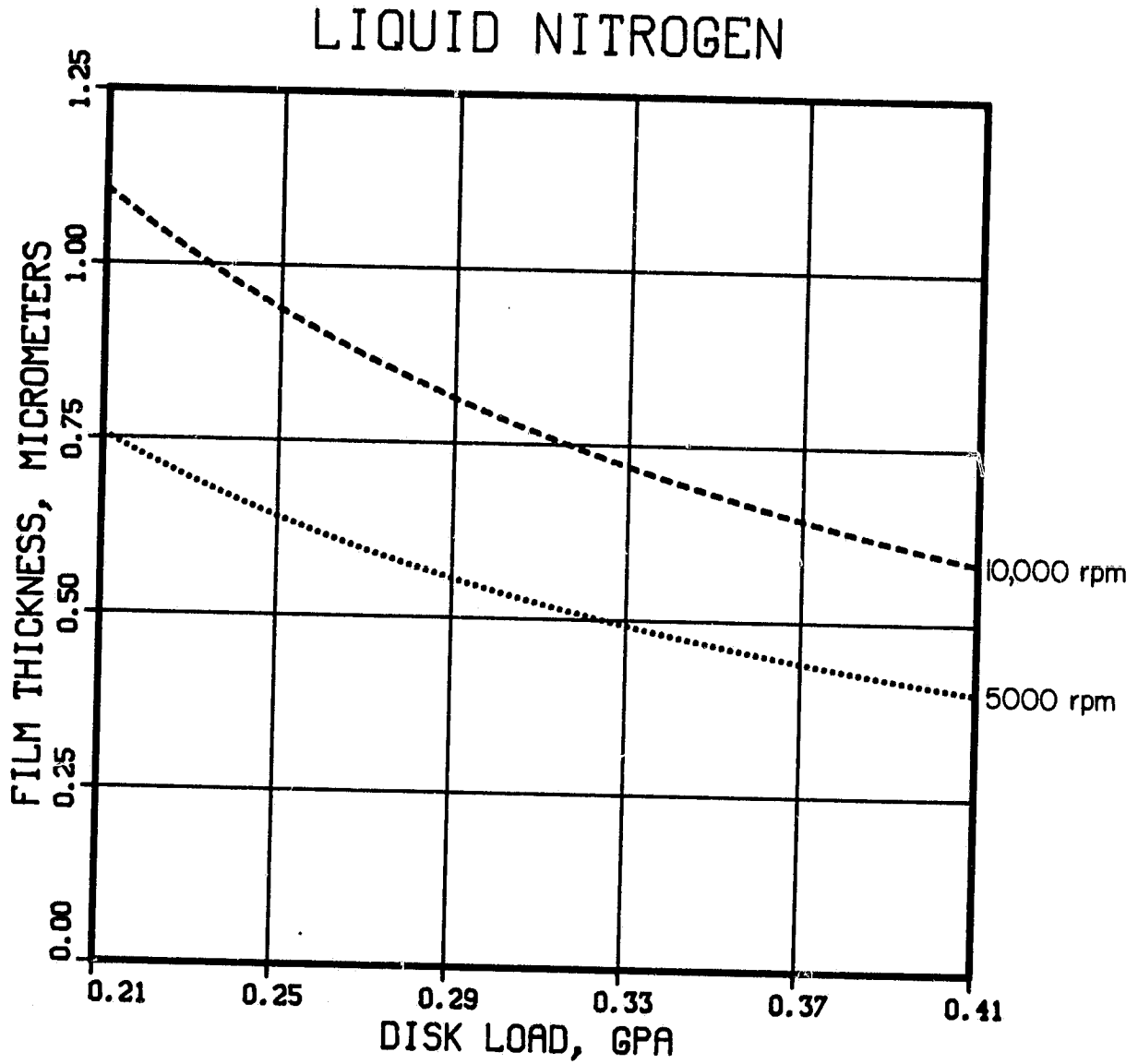


FIGURE 5. REGRESSED FILM THICKNESSES FOR LIQUID NITROGEN
(76.2 mm (3 in.) DIAMETER DISK) METRIC UNITS

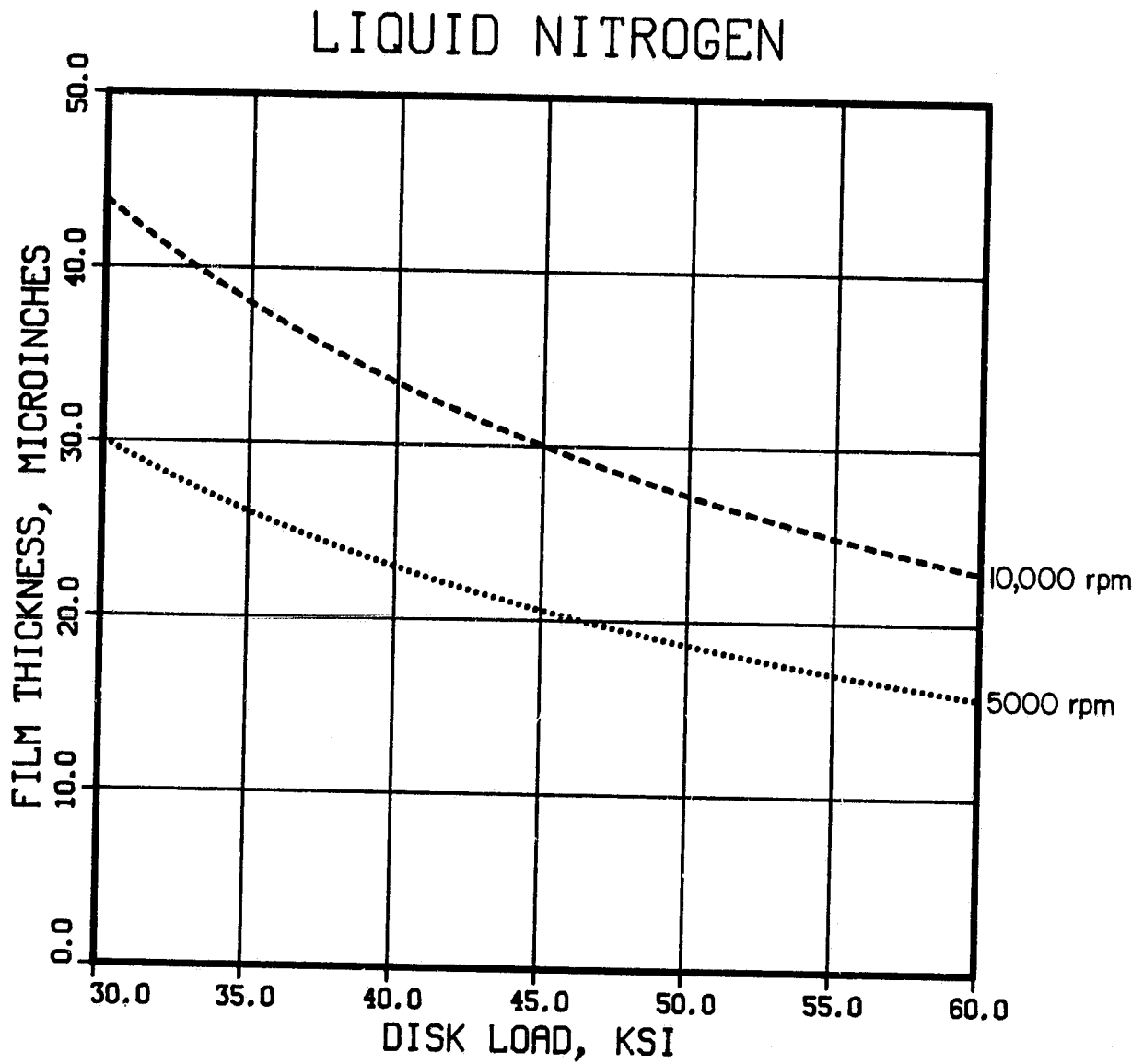


FIGURE 6. REGRESSED FILM THICKNESS FOR LIQUID NITROGEN
(76.2 mm (3 in.) DIAMETER DISK) ENGLISH UNITS

2. Test with smaller diameter or more narrow disks at high loads. For example, experiments can be conducted with 36 mm (1.42 in.) disks at loads to 2 GPa (300 ksi) with the Battelle apparatus. Such tests require very careful realignment of the X-ray system which was beyond the scope of this feasibility study.

In addition to the tests reported herein, several other experiments were attempted to evaluate thermal effects on cryogenic EHD. One experiment involved inducing slip between the disks to heat the disk surfaces. However, slip up to 10% did not appear to alter the film measurement. Also, efforts to alter disk temperature by reducing cryogenic flow only resulted in disk icing, which terminated the tests.

Extrapolation to SSME Pump Bearings

The conditions for the experimental evaluations of film thickness are somewhat different from what would be seen in an actual SSME bearing. For example, the stresses are lower by about a factor of 4 and the speeds are lower by about a factor of 3. One method to extrapolate the data to full engine conditions is to use Equation 3 of the last task order report. This equation could be written in the following form

$$\frac{h_B}{h_D} = \left(\frac{R_{B_r}}{R_D} \right)^{3/11} \left[\frac{(U_1 + U_2)_{B_r}}{(U_1 + U_2)_D} \right]^{8/11} \left(\frac{P_{HD}}{P_{H_{B_r}}} \right)^{10/11}, \quad (1)$$

where

R is the relative radii of the surfaces $\frac{1}{R} = \frac{1}{R_1} + \frac{1}{R_2}$

U is the surface velocity

P_H is the maximum Hertz pressure

B_r subscript means bearing

D subscript means disk

for a bearing

$$U_1 + U_2 = \frac{\omega R}{R_p} [R_p^2 - (R_B \cos \beta)^2] \quad , \quad (2)$$

where

ωR is the bearing angular velocity (rad/sec)

R_p is the radius of pitch

R_B is the ball radius

β is the contact angle.

Typical conditions for a bearing and disk are given in Table 2. Using these conditions with the data of Table 1, the following film thickness would be predicted.

$$h_B = .20 \mu\text{m} (7.7 \mu\text{in.}) @ 1.38 \text{ GPa} (200 \text{ ksi}) \quad , \quad (3)$$

$$h_B = .14 \mu\text{m} (5.3 \mu\text{in.}) @ 2.07 \text{ GPa} (300 \text{ ksi}) \quad . \quad (4)$$

Film thicknesses with a magnitude of greater than $13 \mu\text{m}$ ($5 \mu\text{in.}$) can be sufficient to protect bearing surfaces if the surfaces are very smooth. It would appear then that LN_2 could lubricate a bearing by classical EHD mechanisms.

Analysis of Test Bearings

Portions of three bearings from two SSME high pressure oxygen turbopumps (HPOTP) were received for examination of the wear patterns and estimation of the corresponding responsible loads. Identification of the bearings, the number of starts, and time of running at different power levels is presented in Table 3.

Component Inspection

Examination of the 120-degree segments of the races and four balls from the No. 3 turbine bearing of unit 2209R1 showed evidence of high loads in both the axial and radial direction. As shown in Figure 7, the axial load caused the ball track on the inner race to reach the shoulder and roll a burr

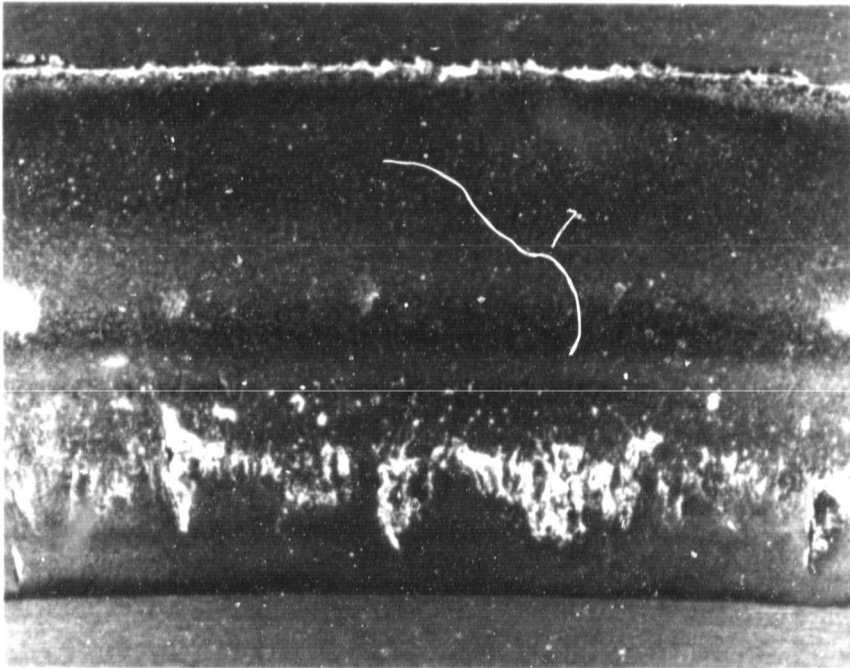
TABLE 2. SUMMARY OF GEOMETRY AND OPERATING CONDITIONS FOR
SSME TURBOPUMP BEARING (7955) AND BATTELLE DISK
APPARATUS

Parameter	Symbol	Units	Assumed Value(s)
Bearing			
Ball Radius	R_B	mm(in.)	6.35 (.25)
Pitch Radius	R_P	mm(in.)	40 (1.57)
Contact Angle	β	degrees	50
Speed	ω	rpm (rad/sec)	30,000 (3141)
Velocity Sum	$U_1 + U_2$	m/sec (ips)	122.5 (4184)
Contact Stress	p_H	GPa (ksi)	1.38 - 2.07 (200 - 300)
Inner Race Radius	R_r	mm(in.)	5.33 (.21)
Disk			
Radius	R_D	mm(in.)	19.06 (.75)
Velocity Sum	$U_1 + U_2$	m/sec (ips)	40 (1570)
Contact Stress	p_H	GPa (ksi)	.21 - .41 (30 - 60)

TABLE 3. IDENTIFICATION AND TIME OF RUNNING ON THREE BEARINGS FROM HPOTP TESTS

Unit No.	Bearing Position No.	Set No.	Starts	Total Time, s	104% Time, s	106% Time, s	109% FPL Time, s	111% Time, s
2209R1	Turbine 3	034	14	3958.4	418	470	2081.7	-
2209R1	Pre-burner 2	952	15	4468.4	418	470	2461.7	-
2111	Turbine 4	021	3	1250	-	-	610	375

ORIGINAL PAGE IS
OF POOR QUALITY



2L404

10x

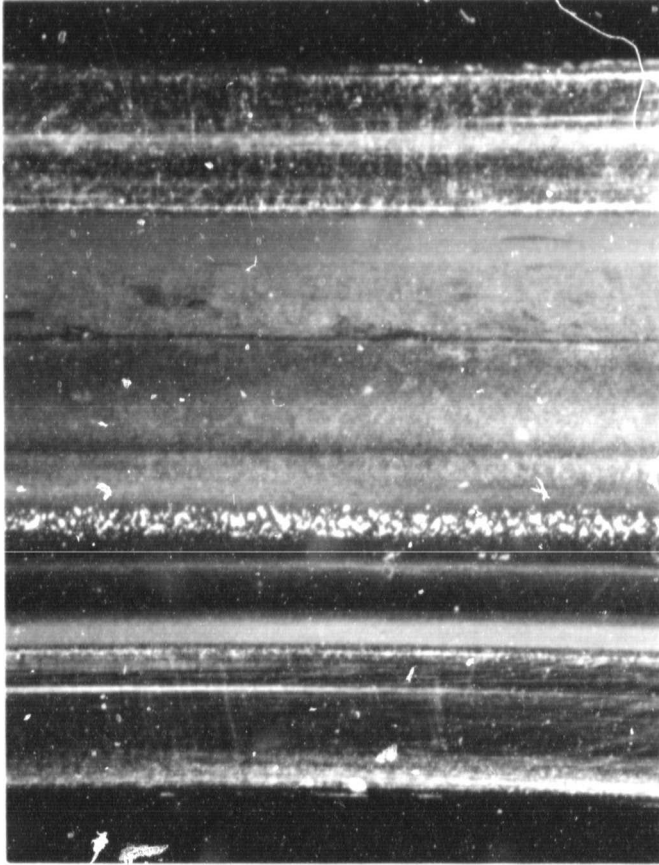
FIGURE 7. ROLLED-OVER SHOULDER (AT TOP OF PHOTO) AND
BAND OF SPALLS ON INNER RACE OF TURBINE
BEARING NO. 3 FROM UNIT 2209R1

at the corner. This portion of the race conformed with the ball radius, which confirmed that the plastic deformation (possibly combined with wear) was a result of a high axial load. The inner race also had a track of fatigue spalls at the radial load (zero contact angle) position, which was slightly skewed in location but otherwise uniform over the 120 degree segment. The band reportedly was continuous around the entire inner race, which is indicative of a high continuous radial load (non synchronous). The balls were uniformly darkened in color and had a nominal diameter of 12.62 mm (0.497 inch), which is 0.08 mm (0.003 inch) under the typical standard diameter. The outer race had a clearly defined dark contact track with a continuous band of spalls near one edge, Figure 8. The location of the spalls was consistent with an axial load on the bearing.

The balls and race segments from the No. 2 preburner bearing from unit 2209R1 had evidence of very high continuous radial loads, but an absence of high axial loads. The inner race had a continuous band of spalls located at the pure radial load (zero contact angle) position. It was reportedly present around the entire circumference. The balls were worn to 11.0 mm (0.434 inch), which was 0.08 to 0.10 mm (0.003 to 0.004 inch) less than the original nominal diameter. The outer race ball track was wide, centrally located, and had a unusual uniform scalloped pattern on one edge, Figure 9. The outer-diameter mounting surface showed evidence of spinning in its housing, Figure 10. This bearing apparently was damaged from a repetitive load (such as high frequency vibration), which scalloped the outer race and caused it to spin in its housing.

The third bearing components available, from turbine bearing No. 4 of unit No. 2111, showed that the bearing had been subjected to a very high axial load and had ball wear, but was free of race spalling. The shoulder of the inner race had a ball-conforming groove, which caused the shoulder to be rolled over into a burr with numerous chips removed. The ball path also extended to the zero-contact-angle position, indicative of high continuous radial loads. There were no spalls present. The ball diameters measured 12.3 to 12.4 mm (0.484 to 0.489 inch) which is 0.41 to 0.28 mm (0.016 to 0.011 inch) under the nominal 12.7 mm (0.500 inch) original diameter. The cage was also available for inspection. It had experienced diametral

ORIGINAL PAGE IS
OF POOR QUALITY

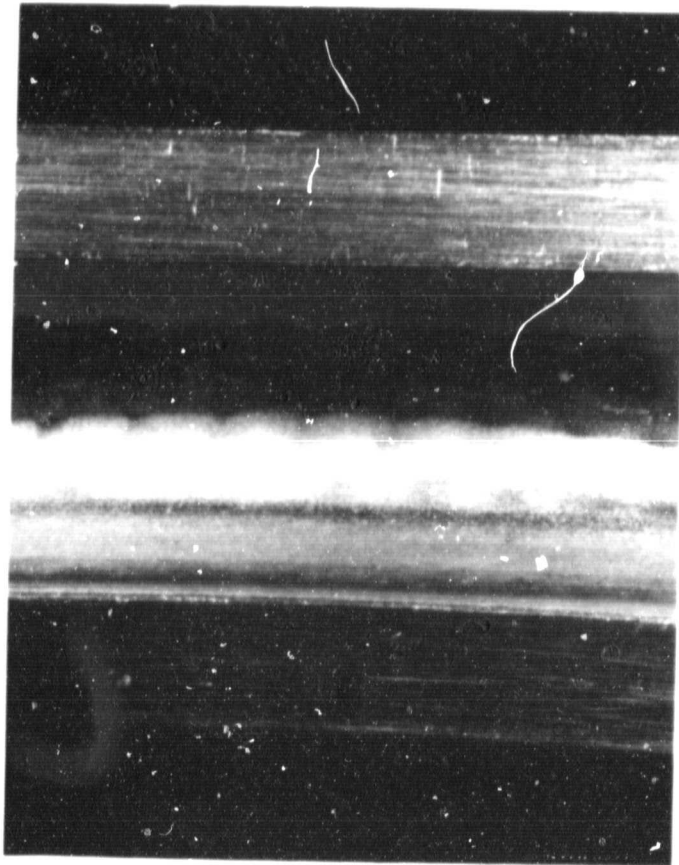


2L405

5x

FIGURE 8. BAND OF SPALLS ON OUTER RACE OF TURBINE
BEARING NO. 3 FROM UNIT 2209R1

ORIGINAL PAGE IS
OF POOR QUALITY

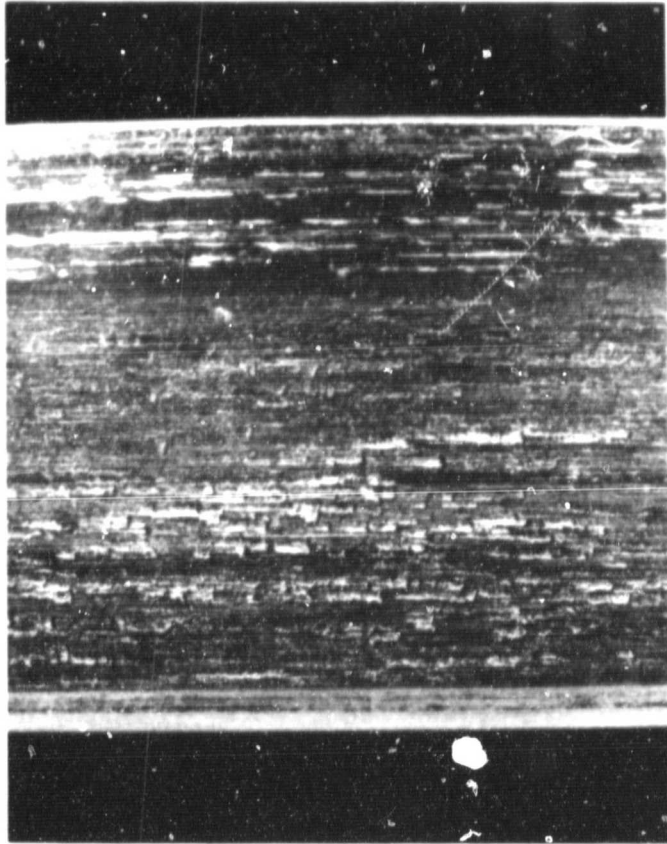


2L403

5x

FIGURE 9. SCALLOPED WEAR PATTERNS ON OUTER RACE OF NO. 2
PREBURNER BEARING FROM UNIT NO. 2209R1

ORIGINAL PAGE IS
OF POOR QUALITY



2L402

5x

FIGURE 10. DAMAGE FROM SPINNING TO THE OUTER DIAMETER OF THE OUTER RACE OF NO. 2 PREBURNER BEARING FROM UNIT NO. 2209R1

pocket wear of 0.99 to 1.2 mm (0.039 to 0.047 inch). The inner guiding surface that had mated with the rolled-over inner-race shoulder had a groove cut approximately 0.3 mm (0.012 inch) deep. In spite of this damage, the cage appeared to be serviceable. The outer race was spall-free and had a wide well defined dark ball path. The width is suggestive of a widely varying load history.

Bearing Load Computations

An attempt was made to determine the likely loads responsible for the race wear patterns observed on the bearings. From previous analyses of the effect of axial loads on the turbine-end bearings of the HPOTP, axial loads of 36,000 to 44,000 N (8,000 to 10,000 lb) are required to cause the shoulder of the inner race to roll over. On this basis, the two turbine-end bearings examined in this task also apparently were subjected to axial loads of this magnitude. Since the bearings were from both positions 3 and 4, the high axial loads are apparently possible in both directions.

The high radial loads responsible for causing operation with a zero contact angle and inner race spalling in this location had not been previously observed on HPOTP bearings by Battelle. Therefore, a series of computations were made to explore the effect of radial load and inner-race growth on contact angle, contact stress, and contact width. The calculations were made using the Battelle bearing dynamics model BASDAP.

Table 4 summarizes the basic input parameters for the SSME HPOTP turbine-end bearings (7955) used in the calculations. Figures 11 through 14 summarize the predictions generated by BASDAP. Figure 11 shows the effect of shaft growth on contact angle. If the shaft grows about 0.25 to 0.3 mm (0.01 to 0.12 inch) as a result of unfavorable thermal effects, the clearance in the bearing is eliminated and the contact angle tends to zero. Likewise, as shown in Figure 12, the contact stresses and contact half widths become very large.

As an externally applied radial load is increased for a given axial preload of 3780 N (850 lb), as shown in Figure 13, the contact angle decreases at the maximum load position. However, the contact angle does not approach

ORIGINAL PAGE IS
OF POOR QUALITY

TABLE 4. ASSUMED DESIGN CONDITIONS FOR HPOTP
TURBINE-END BEARINGS

Parameter		Bearing Type 7955
Ball Diameter	mm(in.)	12.7 (.500)
Pitch Diameter	mm(in.)	81.0 (3.19)
Contact Angle	Degrees	20.5
Inner Race Curvature		.53
Outer Race Curvature		.53
Number of Balls		13
Speed	RPM	30,000

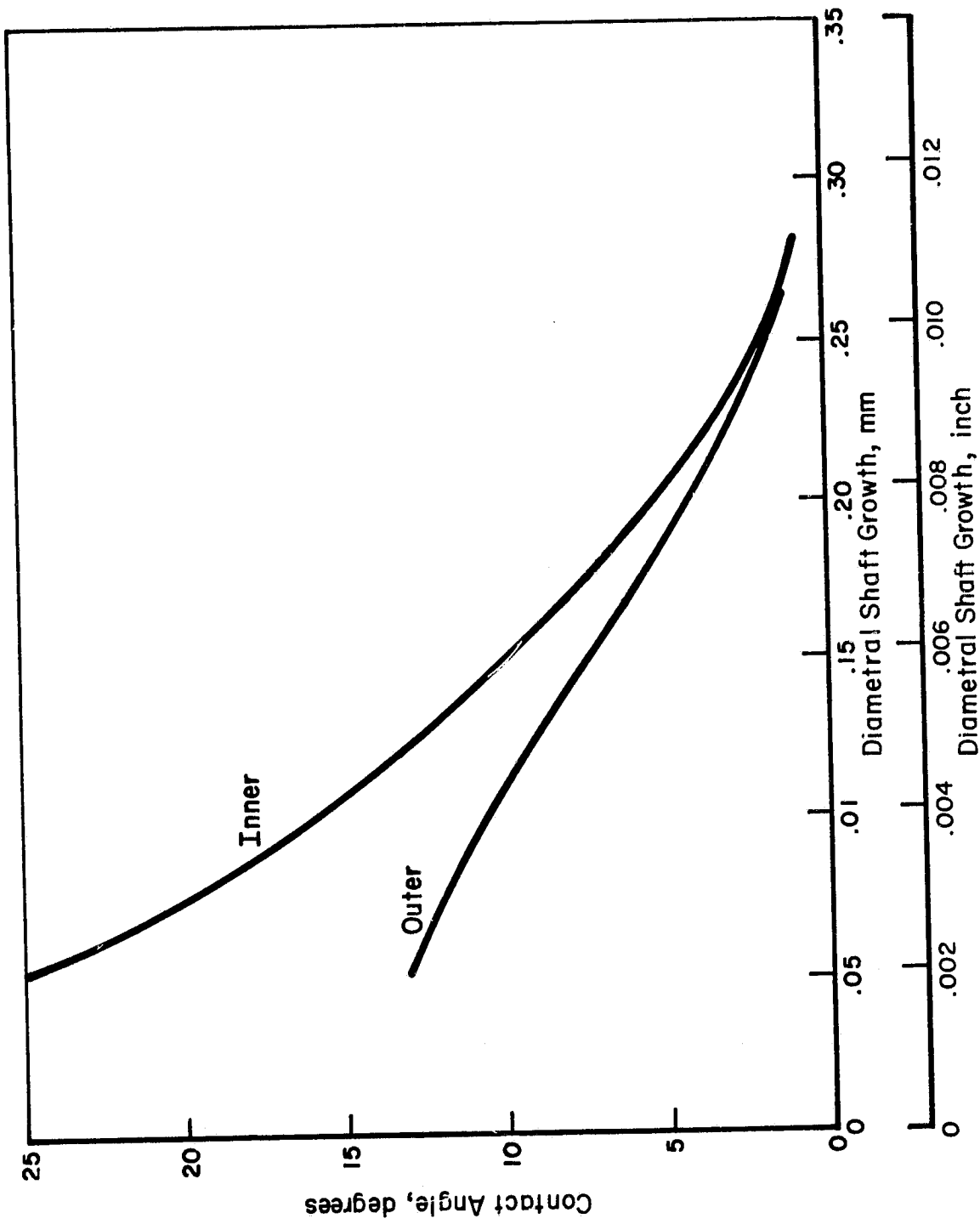


FIGURE 11. CONTACT ANGLE VARIATION FOR SSME HPOTP BEARING (7955) AT 30,000 rpm, 3780 N (850 lb) AXIAL AND NO EXTERNAL RADIAL LOAD

ORIGINAL PAGE IS
OF POOR QUALITY

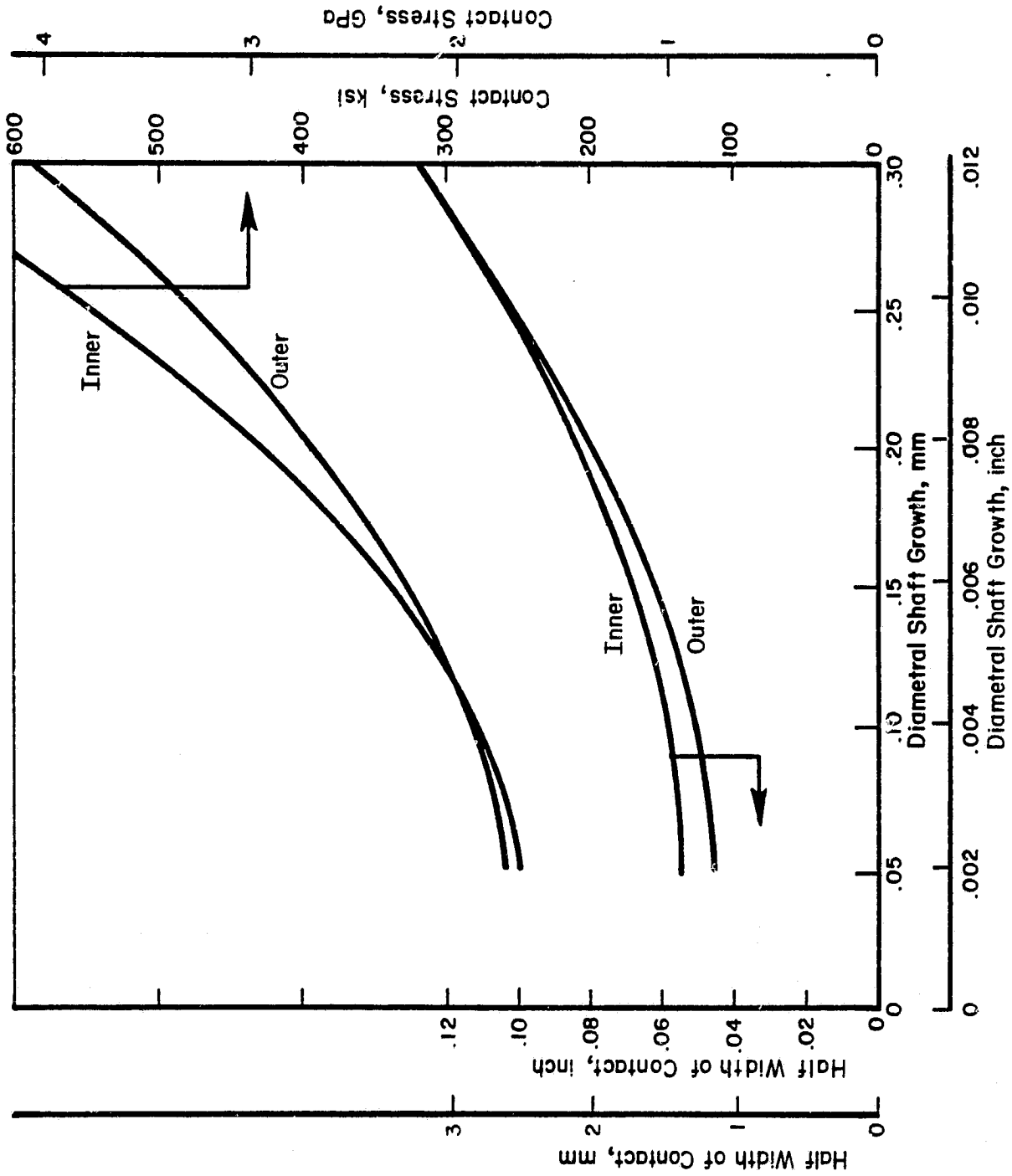


FIGURE 12. CONTACT STRESS AND LENGTH FOR SMME HPOTP BEARING (7955) AT 30,000 rpm, 3780 N (850 lb) AXIAL AND NO RADIAL LOAD

ORIGINAL PAGE 10
OF POOR QUALITY

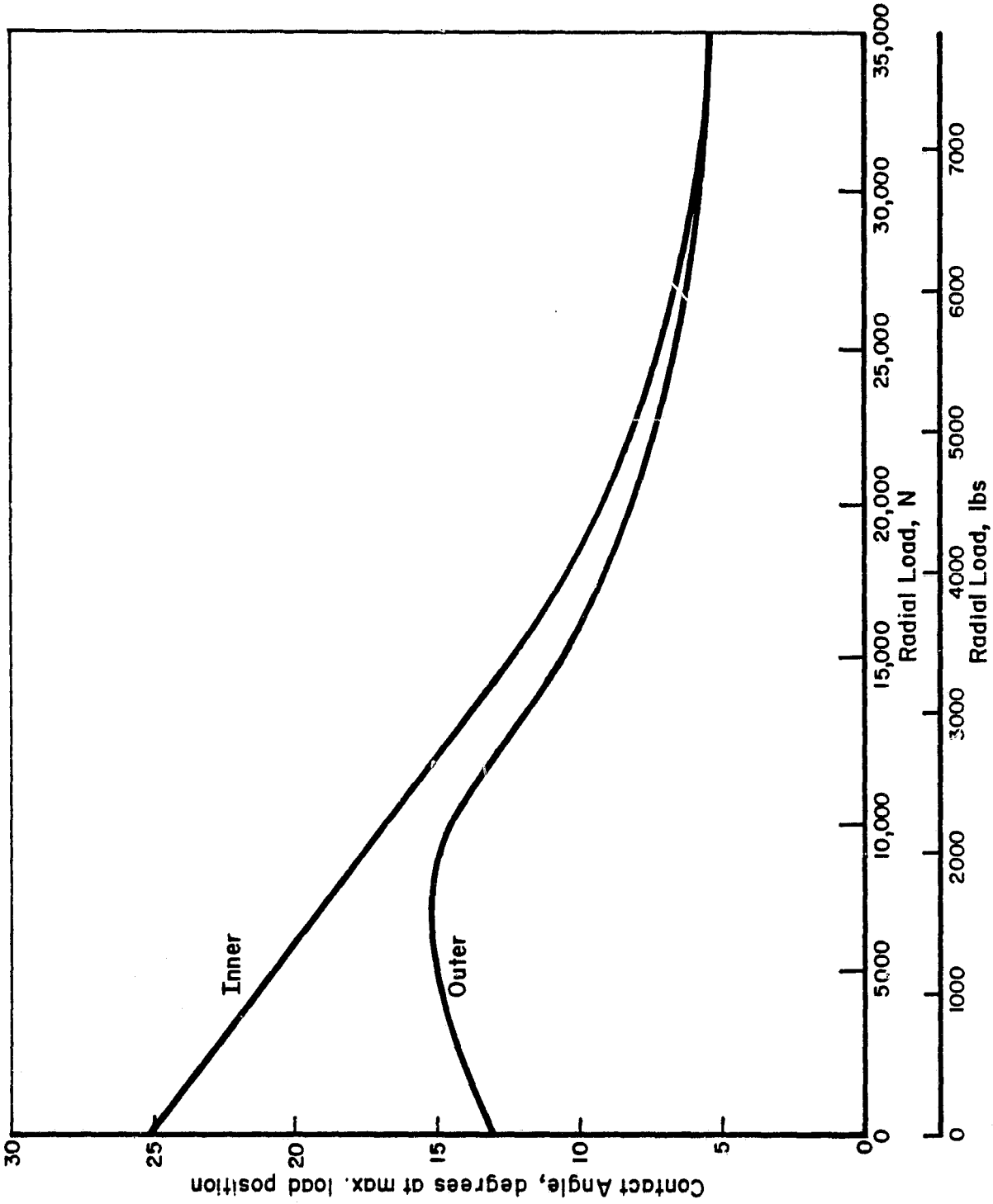


FIGURE 13. CONTACT ANGLE VARIATION WITH RADIAL LOAD AT MAXIMUM LOAD POSITION SSME HPOTP BEARING (7955) AT 30,000 rpm AND 3780 N (850 lb) AXIAL LOAD

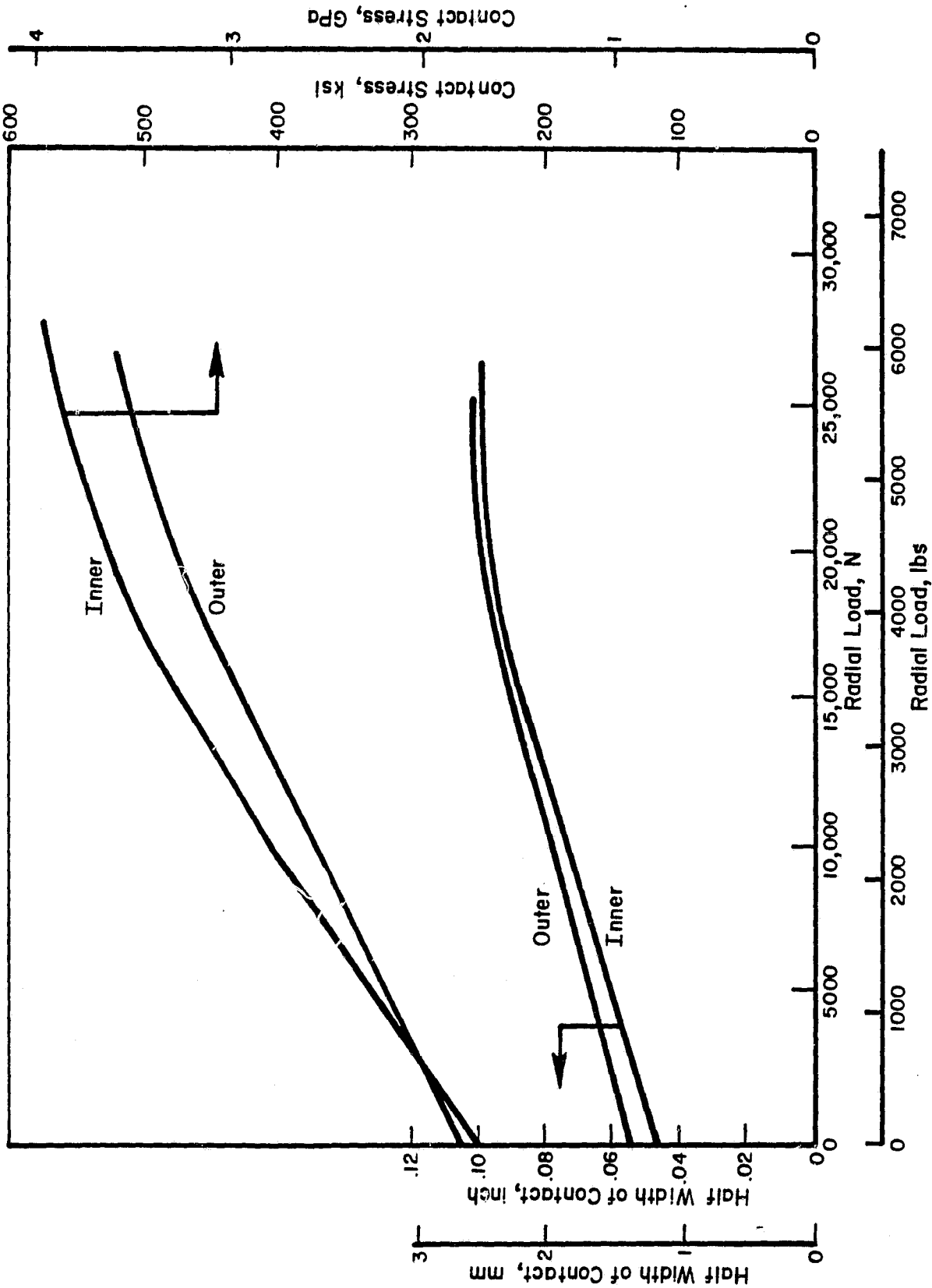


FIGURE 14. CONTACT STRESS AND HALF-WIDTH VARIATION WITH RADIAL LOAD AT MAXIMUM LOAD POSITION FOR SSME HPOTP TURBOPUMP BEARING (7955) AT 30,000 rpm AND 3780 N (850 lb) AXIAL LOAD

zero even at loads as high as 35,000 N (8,000 lb). The corresponding contact stresses and contact half widths are shown in Figure 14. The contact stresses rise to a very high value as the radial load is increased to 35,000 N (8,000 lb). The calculations also showed that on the outer race at the minimum load position the contact angle tends to zero with radial loads greater than 4,400 N (1,000 lb). This is the result of centrifugal loading of the balls when the combination of axial and radial loads relieve the ball load in the minimum load position. The contact stress due to centrifugal loading is 1.42 GPa (207 ksi) and the half width is 1.1 mm (0.042 inch).

Applying these calculated results of the effect of inner race growth and radial loads on resulting stresses and contact angles to the two HPOTP turbine bearings, the low contact angles and high continuous radial loads are best explained by inner race growth. Since the wear patterns on the inner race were continuous, the loads could not have been synchronous (out of balance) loads. Since the outer race wear paths were also continuous, the radial load could not have been externally applied (there is also no logical source of a continuous radial load exceeding 35,000 N (8,000 lb)). Therefore, a run-away thermal growth of the inner race is the likely source of the very high internal loads experienced. A diametral growth of .025 to 0.3 mm (0.010 to 0.012 inch) would be required to reach the zero contact angle observed on the races. However, such growth causes intolerably high contact stresses exceeding 3.5 GPa (500,000 ksi). Therefore, the bearing races experienced spalling and the balls wore to relieve the internal loads.

Calculating Units

Since the bearing drawing and all input data provided by NASA were in English units, all calculations were performed in English units. Therefore, the SI units presented in this report were converted from English units.